

The quantum needle of the avian magnetic compass

Hamish G. Hiscock^{a,1}, Susannah Worster^{a,1}, Daniel R. Kattinig^a, Charlotte Steers^a, Ye Jin^a, David E. Manolopoulos^a, Henrik Mouritsen^{b,c}, and P. J. Hore^{a,2}

^aDepartment of Chemistry, Physical & Theoretical Chemistry Laboratory, University of Oxford, Oxford OX1 3QZ, United Kingdom; ^bInstitut für Biologie und Umweltwissenschaften, Carl von Ossietzky Universität Oldenburg, 26111 Oldenburg, Germany; and ^cResearch Centre for Neurosensory Sciences, University of Oldenburg, 26111 Oldenburg, Germany

Edited by Michael L. Klein, Temple University, Philadelphia, PA, and approved March 1, 2016 (received for review January 8, 2016)

Migratory birds have a light-dependent magnetic compass, the mechanism of which is thought to involve radical pairs formed photochemically in cryptochrome proteins in the retina. Theoretical descriptions of this compass have thus far been unable to account for the high precision with which birds are able to detect the direction of the Earth's magnetic field. Here we use coherent spin dynamics simulations to explore the behavior of realistic models of cryptochrome-based radical pairs. We show that when the spin coherence persists for longer than a few microseconds, the output of the sensor contains a sharp feature, referred to as a spike. The spike arises from avoided crossings of the quantum mechanical spin energy-levels of radicals formed in cryptochromes. Such a feature could deliver a heading precision sufficient to explain the navigational behavior of migratory birds in the wild. Our results (i) afford new insights into radical pair magnetoreception, (ii) suggest ways in which the performance of the compass could have been optimized by evolution, (iii) may provide the beginnings of an explanation for the magnetic disorientation of migratory birds exposed to anthropogenic electromagnetic noise, and (iv) suggest that radical pair magnetoreception may be more of a quantum biology phenomenon than previously realized.

magnetic compass | magnetoreception | migratory birds | quantum biology | radical pair mechanism

Migratory birds have a light-dependent magnetic compass (1–4). The primary sensory receptors are located in the eyes (2, 3, 5–7), and directional information is processed bilaterally in a small part of the forebrain accessed via the thalamofugal visual pathway. The evidence currently points to a chemical sensing mechanism based on photo-induced radical pairs in cryptochrome flavoproteins in the retina (8–18). Anisotropic magnetic interactions within the radicals are thought to give rise to intracellular levels of a cryptochrome signaling state that depend on the orientation of the bird's head in the Earth's magnetic field (8, 9, 19). In support of this proposal, the photochemistry of isolated cryptochromes in vitro has been found to respond to applied magnetic fields in a manner that is quantitatively consistent with the radical pair mechanism (15). Aspects of the radical pair hypothesis have also been explored in a number of theoretical studies, the majority of which have concentrated on the magnitude of the anisotropic magnetic field effect (9, 10, 16, 17, 19–27). Very little attention has been devoted to the matter we address here: the precision of the compass bearing available from a radical pair sensor (28).

To migrate successfully over large distances, it is not sufficient simply to distinguish north from south (or poleward from equatorward) (29). A bar-tailed godwit (*Limosa lapponica baueri*), for example, was tracked by satellite flying from Alaska to New Zealand in a single 11,000-km nonstop flight across the Pacific Ocean (30). A directional error of more than a few degrees could have been fatal. Because the magnetic compass seems to be the dominant source of directional information (31), and the only compass available at night under an overcast (but not completely dark) sky, migratory birds must be able to determine their flight direction with high precision using their magnetic compass. Studies have shown that migratory songbirds can detect the axis of the magnetic field lines with an accuracy better than 5° (32, 33). Any plausible magnetoreception

hypothesis must be able to explain how such a directional precision can be achieved. Previous simulations of radical pair reactions (9, 10, 17, 20, 21) show only a weak dependence on the direction of the geomagnetic field and therefore cannot straightforwardly account for the magnetic orientation of birds in the wild.

Theoretical treatments of radical pair-based magnetoreception typically involve simulations of the quantum spin dynamics of short-lived radicals in Earth strength (~50 μT) magnetic fields (9, 10, 17). The general aim is to determine how the yield of a reaction product depends on the orientation of the reactants with respect to the magnetic field axis. A crucial element in all such calculations is the presence of nuclear spins whose hyperfine interactions are the source of the magnetic anisotropy (8, 16). Most studies have focused on idealized spin systems comprising the two electron spins, one on each radical, augmented by one or two nuclear spins (9, 21–27, 34). Only a handful has attempted to deal with realistic, multinuclear radical pairs (10, 16, 17, 20). The other critical ingredient in such simulations is the lifetime of the electron spin coherence: if the spins dephase completely before the radicals have a chance to react, there can be no effect of an external magnetic field (35). Several studies have assumed, explicitly or implicitly, that the spin coherence persists for about a microsecond, i.e., the reciprocal of the electron Larmor frequency (1.4 MHz) in a 50-μT field (9, 10, 17, 20). Either because the spin system was grossly oversimplified (9, 21–27, 34), or because of this restriction on the spin coherence time, previous theoretical treatments have generally predicted the reaction yield to be a gently varying (often approximately sinusoidal) function of the orientation of the radical pair in the geomagnetic field. Although capable of delivering information on the direction of the field, such a compass would not provide a precise heading. A

Significance

Billions of birds fly thousands of kilometers every year between their breeding and wintering grounds, helped by an extraordinary ability to detect the direction of the Earth's magnetic field. The biophysical sensory mechanism at the heart of this compass is thought to rely on magnetically sensitive, light-dependent chemical reactions in cryptochrome proteins in the eye. Thus far, no theoretical model has been able to account for the <5° precision with which migratory birds are able to detect the geomagnetic field vector. Here, using computer simulations, we show that genuinely quantum mechanical, long-lived spin coherences in realistic models of cryptochrome can provide the necessary precision. The crucial structural and dynamical molecular properties are identified.

Author contributions: P.J.H. designed research; H.G.H., S.W., D.R.K., C.S., and Y.J. performed research; D.E.M., H.M., and P.J.H. wrote the paper; and C.S. and Y.J. performed preliminary calculations.

The authors declare no conflict of interest.

This article is a PNAS Direct Submission.

¹H.G.H. and S.W. contributed equally to this work.

²To whom correspondence should be addressed. Email: peter.hore@chem.ox.ac.uk.

This article contains supporting information online at www.pnas.org/lookup/suppl/doi:10.1073/pnas.1600341113/-DCSupplemental.

more sharply peaked dependence on the field direction would be needed to achieve a compass bearing with an error of 5° or less.

Here, we explore the behavior of cryptochrome-inspired radical pairs with multinuclear spin systems and long-lived ($>1 \mu\text{s}$) spin coherence. We conclude that there is ample scope for a cryptochrome-based radical pair compass to have evolved with a heading precision sufficient to explain the navigational behavior of migratory birds both in the laboratory and in the wild.

Results

Spin Dynamics Simulations. Product yields of radical pair reactions were calculated as described elsewhere (10, 16, 36–38) by solving a Liouville equation containing (i) the internal magnetic (hyperfine) interactions of the electron spin with the nuclear spins in each radical, (ii) the magnetic (Zeeman) interactions of the two electron spins with the external magnetic field, and (iii) appropriate spin-selective reactions of the singlet and triplet states of the radical pair.

As a starting point, we modeled $[\text{FAD}^{\bullet-} \text{TrpH}^{\bullet+}]$, the radical pair that is responsible for the magnetic sensitivity of isolated cryptochrome molecules in vitro (15). It consists of the radical anion of the noncovalently bound flavin adenine dinucleotide (FAD) cofactor and the radical cation of the terminal residue of

the “tryptophan (Trp) triad” electron transfer chain within the protein (39–41). All calculations were performed in a coordinate system aligned with the tricyclic flavin ring system (Fig. 1A): x and y are, respectively, the short and long in-plane axes, and z is normal to the plane. Hyperfine interaction tensors were calculated by density functional theory (SI Appendix, Section S1). Following Lee et al. (16), the 14 largest hyperfine interactions, 7 in $\text{FAD}^{\bullet-}$ and 7 in $\text{TrpH}^{\bullet+}$, were included (see SI Appendix, Section S2 for additional simulations including up to 22 nuclear spins.) A magnetic field strength of $50 \mu\text{T}$ was used throughout. The relative orientation of the two radicals was that of FAD and Trp-342 in *Drosophila melanogaster* cryptochrome (Protein Data Bank ID code 4GU5) (SI Appendix, Section S1) (42, 43). The initial state of the spin system was a pure singlet. Two approximations (SI Appendix, Sections S3 and S4) were introduced to make simulations of the 16-spin system computationally tractable (9): (i) exchange and dipolar interactions between the radicals were assumed to be negligible, and (ii) the singlet and triplet states were assumed to react to form distinct products with identical first order rate constants, k . The lifetime of the radical pair, τ , is defined as the reciprocal of k . As a measure of the available directional information, we calculated Φ_S , the fractional yield of the

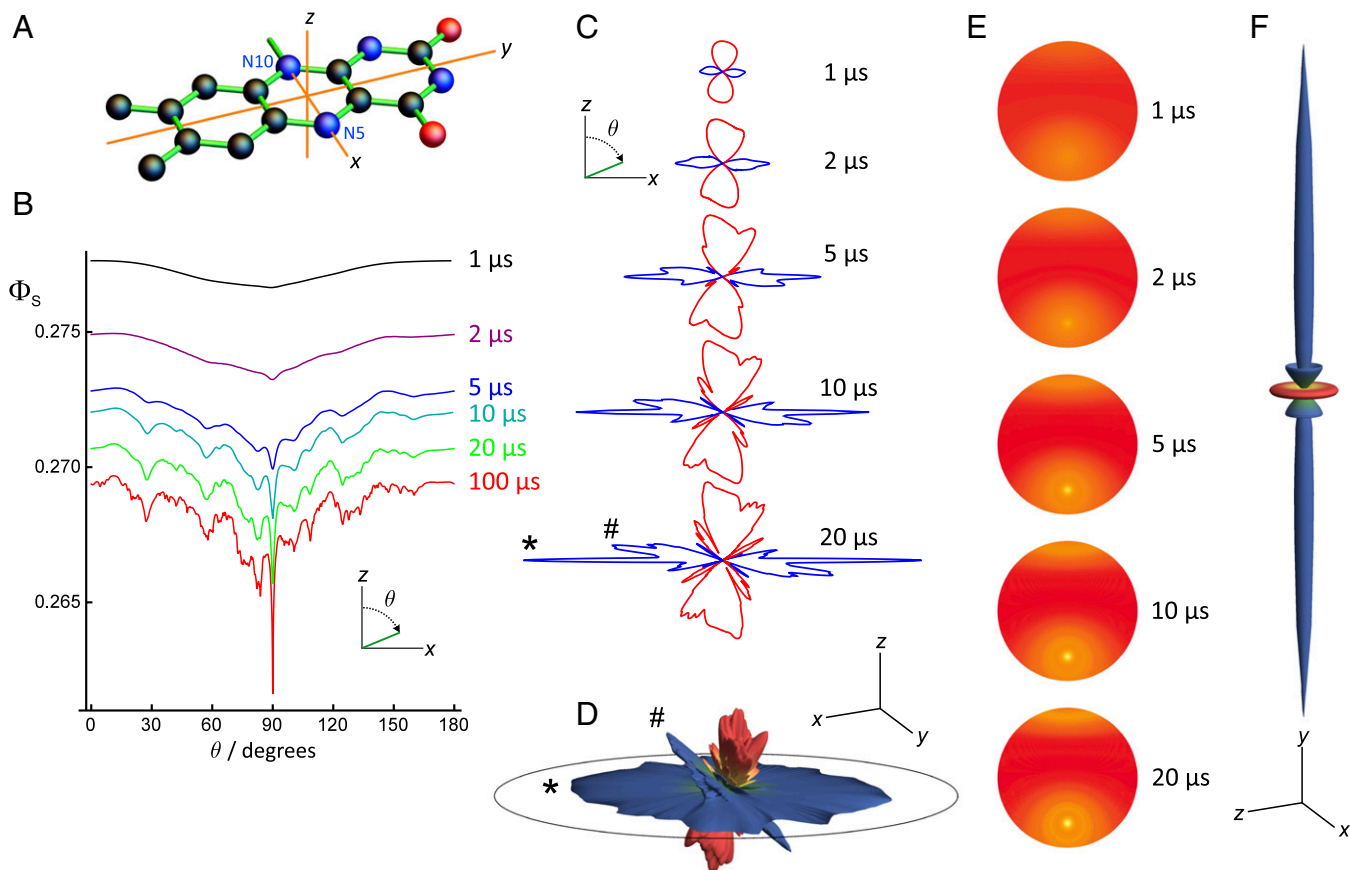


Fig. 1. Reaction yields of a $[\text{FAD}^{\bullet-} \text{TrpH}^{\bullet+}]$ radical pair. (A) The axis system used in the simulations superimposed on the tricyclic flavin ring system. (B) The variation of Φ_S with θ for radical pairs with lifetimes between 1 and $100 \mu\text{s}$. For clarity, two of the traces have been offset vertically: by -0.001 (light green) and -0.002 (red). θ specifies the direction of the magnetic field in the xz plane of the flavin. (C) The same data as in B (1- to $20\text{-}\mu\text{s}$ lifetimes) presented as 2D polar plots. In each case, only the anisotropic part of Φ_S is shown, with red and blue indicating values, respectively, larger and smaller than the isotropic value. The five plots are drawn on the same scale. The blue features at $\theta = \pm 90^\circ$ (labeled * in the $20\text{-}\mu\text{s}$ plot) are the spikes. (D) The anisotropic part of Φ_S ($10\text{-}\mu\text{s}$ lifetime) presented as a 3D polar plot. A circle in the xy plane ($\theta = 90^\circ$) is included as a guide to the eye. The blue disk in the xy plane (labeled *) gives rise to the spike. The smaller blue disk, labeled # (also in C), angled at $\sim 40^\circ$ to the xy plane, comes principally from the N1 indole nitrogen of $\text{TrpH}^{\bullet+}$. Its tilt reflects the orientation of the indole group of the tryptophan relative to the flavin (42, 43). (E) Visual modulation patterns calculated from Φ_S (1- to $20\text{-}\mu\text{s}$ lifetimes) representing the directional information available from an array of cryptochrome-containing magnetoreceptor cells distributed around the retina. The bright spot in the lower half of the pattern arises from the spike. (F) 3D polar plot of Φ_S ($10\text{-}\mu\text{s}$ lifetime) averaged over a 360° rotation around an axis in the xy plane. This object has been rotated by 90° relative to D and scaled up by a factor of 2.1. The patterns in E were calculated using the same averaging procedure (SI Appendix, Section S6).

product formed from the singlet state of the radical pair after the reactions have proceeded to completion (10, 16). Spin relaxation processes were not included in the initial simulations. Further details are given in the *SI Appendix, Section S5*.

Flavin-Tryptophan Radical Pair. Fig. 1*B* shows the variation of Φ_S for $[\text{FAD}^{\bullet-} \text{TrpH}^{\bullet+}]$ as the direction of a 50- μT magnetic field, specified by the angle θ , is rotated in the zx plane of the flavin. When $\theta = 0$, the field is parallel to the flavin z axis (Fig. 1*A*). With a lifetime $\tau = 1 \mu\text{s}$, Φ_S exhibits a shallow minimum around $\theta = 90^\circ$ and maxima near 0° and 180° , as found previously (16). Shorter lifetimes gave even weaker angular variation. As the lifetime is prolonged from 1 μs toward 100 μs , the dependence of Φ_S on θ becomes increasingly structured, and a prominent spike emerges, strengthens, and narrows. Centered accurately at $\theta = 90^\circ$, this feature occurs when the magnetic field is in the plane of the flavin ring system (parallel to the x axis). As τ is increased beyond 100 μs , the only change is that the spike grows (by roughly a factor of 3 as $\tau \rightarrow \infty$).

The anisotropy of Φ_S can be seen more clearly from polar plots of the same data (Fig. 1*C*) after subtraction of the isotropic components. As the lifetime is prolonged, the anisotropy grows, and Φ_S depends more strongly on θ . As expected from time-reversal symmetry, Φ_S is invariant to inversion of the direction of the magnetic field, a property shared by the avian magnetic compass (29). Very similar behavior was found when the magnetic field was rotated in the molecular zy plane. In fact, Φ_S has roughly axial symmetry around the molecular z axis, apart from a tilted feature arising predominantly from the indole nitrogen of $\text{TrpH}^{\bullet+}$, as may be seen from the 3D polar plot in Fig. 1*D* ($\tau = 10 \mu\text{s}$). The spikes in Fig. 1*B* and *C* at $\theta = 90^\circ$ are, in fact, cross-sections through the thin equatorial disk produced when the magnetic field axis is close to the xy plane of the flavin (Fig. 1*D*).

Fig. 1*E* shows “visual modulation patterns” (9, 19, 28) calculated for the same radical pair as Fig. 1*B–D* (details in *SI Appendix, Section S6*). They are representations of a bird’s perception of the directional information delivered by an array of cryptochrome-containing magnetoreceptor cells distributed around the retina: in this case, for a bird in the northern hemisphere looking horizontally toward magnetic north in a 50- μT magnetic field with a 66° inclination. As the lifetime τ is prolonged, and the spike becomes stronger, the spot that indicates the axis of the geomagnetic field

lines becomes more intense and less diffuse. It is not hard to imagine that the patterns in Fig. 1*E* for $\tau \geq 5 \mu\text{s}$ would give more precise compass headings than that for $\tau = 1 \mu\text{s}$.

Finally, a degree of rotational disorder among the magnetoreceptor cells (19, 28) can be modeled by averaging the polar plot in Φ_S (Fig. 1*D*) over a 360° rotation around a chosen axis (*SI Appendix, Section S6*). If this axis is in the xy plane of the flavin, the thin blue equatorial disk in Fig. 1*D* turns into the needle-shaped object (Fig. 1*F*; $\tau = 10 \mu\text{s}$) that appears to be ideal for determining a precise compass bearing. As mentioned above, a radical pair sensor is an inclination compass rather than a polarity compass so that the resemblance of Fig. 1*F* to a magnetized compass needle should not be taken too literally.

Origin of the Spike in Φ_S . The approximate axial symmetry of Φ_S for $\tau = 1 \mu\text{s}$ (Fig. 1*C*) has been noted before and was attributed principally to the two nitrogens, N5 and N10, in the central ring of the $\text{FAD}^{\bullet-}$ radical (10, 16). N5 and N10 are the only nuclei in $[\text{FAD}^{\bullet-} \text{TrpH}^{\bullet+}]$ with hyperfine tensors that, like Φ_S , are approximately axially symmetric around the flavin z axis. It therefore seems probable that they also play a role in creating the spike that arises when $\tau > 5 \mu\text{s}$.

This prediction is confirmed by Fig. 2*A*, which shows Φ_S for a very slightly modified version of $[\text{FAD}^{\bullet-} \text{TrpH}^{\bullet+}]$. The z components of the hyperfine interactions of N5 and N10 in flavin radicals are large, and the x and y components have small but nonzero absolute values (*SI Appendix, Section S7*). The calculated principal values of the two interactions are $(A_{xx}, A_{yy}, A_{zz}) = (-0.087, -0.100, 1.757)$ mT for N5 and $(-0.014, -0.024, 0.605)$ mT for N10 (*SI Appendix, Section S1*; here 1 mT corresponds to 28 MHz). When A_{xx} and A_{yy} for either N5 or N10 were set to zero, the spike was attenuated by 60–70%; when A_{xx} and A_{yy} for both nitrogens were set to zero, the spike disappeared (Fig. 2*A*). The rest of Φ_S remained essentially unchanged. The strong, sharp component of Φ_S for $[\text{FAD}^{\bullet-} \text{TrpH}^{\bullet+}]$ therefore owes its existence, at least in part, to the form of the hyperfine tensors of N5 and N10 in the flavin radical, i.e., large A_{zz} and small but nonzero $|A_{xx}|$ and $|A_{yy}|$.

SI Appendix, Section S8 contains an analysis that unambiguously attributes the thin equatorial disk in Fig. 1*D* to avoided crossings of the quantum mechanical energy levels of the radical pair spin Hamiltonian as a function of the magnetic field direction and predicts that the line shape of a cross-section

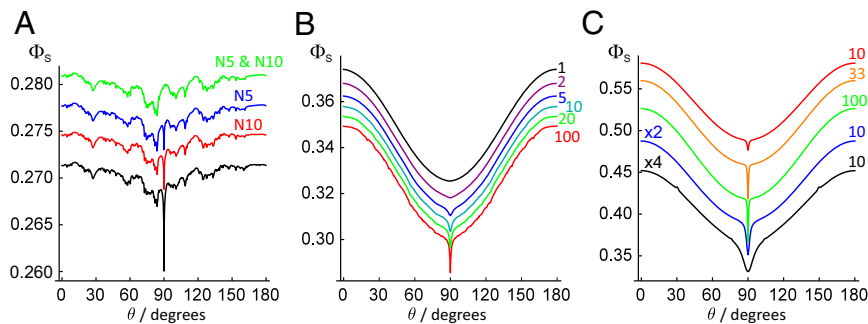


Fig. 2. Reaction yields of various radical pairs. (A) Φ_S for a $[\text{FAD}^{\bullet-} \text{TrpH}^{\bullet+}]$ radical pair in which the transverse principal components of selected nitrogen hyperfine interactions (A_{xx} and A_{yy}) were set to zero: for N5 (blue), N10 (red), and both N5 and N10 (green). Φ_S for the unmodified $[\text{FAD}^{\bullet-} \text{TrpH}^{\bullet+}]$ is shown in black. In all cases, $\tau = 1 \text{ ms}$. For clarity, three of the traces have been offset vertically by 0.006 (green) and 0.003 (blue and red). (B) Φ_S for a $[\text{FAD}^{\bullet-} \text{Y}^{\bullet}]$ radical pair in which radical Y^{\bullet} contains a single ^{14}N nucleus with an axial hyperfine tensor with principal components $(A_{xx}, A_{yy}, A_{zz}) = (0.0, 0.0, 1.0812)$ mT (modeled on N1 in $\text{TrpH}^{\bullet+}$). The radical pair lifetimes are as indicated (1–100 μs). The angle between the z axes of Y^{\bullet} and $\text{FAD}^{\bullet-}$ was 45° ; the intensity of the spike was found to decrease smoothly to zero as this angle was increased from 0° to 90° . For clarity, the five traces for $\tau < 100 \mu\text{s}$ have been offset vertically, from top to bottom, by 0.020, 0.016, 0.012, 0.008, and 0.004 respectively. (C) Φ_S for toy radical pairs, $[\text{X}^{\bullet} \text{Y}^{\bullet}]$. For the red, orange and green traces, X^{\bullet} contains a single ^{14}N hyperfine tensor with principal components $(A_{xx}, A_{yy}, A_{zz}) = (-0.0989, -0.0989, 1.7569)$ mT. For the blue and black traces, $(A_{xx}, A_{yy}, A_{zz}) = (-0.2, -0.2, 1.7569)$ and $(-0.4, -0.4, 1.7569)$ mT, respectively. In all five cases, Y^{\bullet} contains a single ^{14}N nucleus with an axial hyperfine interaction: $(A_{xx}, A_{yy}, A_{zz}) = (0.0, 0.0, 1.0812)$ mT. The two hyperfine tensors have parallel z axes. The radical pair lifetimes are as indicated (10, 33.3, 100 μs); $\times 2$ and $\times 4$ indicate the doubling and quadrupling of A_{xx} and A_{yy} in X^{\bullet} . For clarity, three of the traces have been offset vertically by 0.03 (green) and 0.06 (orange and red).

through the disk (i.e., the spike) will be an upside-down Lorentzian. When A_{xx} and A_{yy} for both nitrogens are set to zero, the avoided crossings become level crossings and the spike vanishes.

Simpler Flavin-Containing Radical Pairs. To obtain further insight into the origin of the spike, simulations were performed for three radical pairs related to $[\text{FAD}^{\bullet-} \text{TrpH}^{\bullet+}]$ (1). When the $\text{TrpH}^{\bullet+}$ radical was replaced by a hypothetical radical that had no hyperfine interactions, Φ_S was found to vary smoothly and approximately sinusoidally with θ and barely changed as τ was increased from 1 to 100 μs (*SI Appendix, Section S9*) (2). This pattern (gentle, smooth θ dependence, no spike) persisted when a single isotropic hyperfine interaction was present in the second radical (*SI Appendix, Section S9*) (3). However, when the second radical contained an axially anisotropic hyperfine interaction with $A_{xx} = A_{yy} = 0$ or $A_{xx} = A_{yy} \neq 0$, the spike at $\theta = 90^\circ$ reappeared and, as in Fig. 1B, strengthened with increasing lifetime (Fig. 2B). From this and other simulations of flavin-containing radical pairs, it appears that an additional condition for the existence of the spike is that the radical that partners the $\text{FAD}^{\bullet-}$ should have at least one nucleus with an anisotropic hyperfine interaction. This condition is amply fulfilled by $\text{TrpH}^{\bullet+}$, in which the indole nitrogen and the aromatic hydrogens all interact anisotropically with the electron spin (16).

A Toy Radical Pair. To confirm and further explore these conclusions, we devised a “toy” radical pair, with a smaller, more manageable spin system, that behaves qualitatively like $[\text{FAD}^{\bullet-} \text{TrpH}^{\bullet+}]$. One radical (X^\bullet) had a single nitrogen with a hyperfine tensor similar to that of the N5 in $\text{FAD}^{\bullet-}$. The other (Y^\bullet) had a single nitrogen with an axial hyperfine tensor modeled on the indole nitrogen in $\text{TrpH}^{\bullet+}$. Like $[\text{FAD}^{\bullet-} \text{TrpH}^{\bullet+}]$, $[\text{X}^\bullet \text{Y}^\bullet]$ shows a spike at $\theta = 90^\circ$ superimposed on a rolling background (Fig. 2C). The spike became more pronounced when either the lifetime was prolonged or the amplitudes of the small transverse hyperfine components in X^\bullet were increased. For example, doubling A_{xx} and A_{yy} when $\tau = 10 \mu\text{s}$ increased the amplitude of the spike by about the same amount as increasing τ from 10 to 33 μs without changing A_{xx} and A_{yy} (Fig. 2C).

Spin Relaxation in the Toy Radical Pair. Of course, the spin coherence does not persist indefinitely but inevitably relaxes toward the equilibrium state in which all spin correlation has vanished. The rate of this process is highly relevant because there can be no magnetic field effect if the spin system equilibrates before the radicals react. The dominant spin relaxation pathways in a cryptochrome-based radical pair probably arise from modulation of hyperfine interactions by low-amplitude stochastic librational motions of the radicals within their binding pockets in the protein. The approach to equilibrium is likely to be highly complex for realistic radicals undergoing realistic motions especially because the external magnetic field is weaker than many of the hyperfine interactions. In general, one can expect a multitude of relaxation pathways, at a variety of rates, not all of which necessarily degrade the performance of the radical pair as a compass sensor (44).

To explore the conditions necessary for the spike to survive in the presence of molecular motion, we studied a simple model of the microscopic dynamics of the $\text{FAD}^{\bullet-}$ radical in cryptochrome. The tricyclic isoalloxazine moiety was allowed to undergo rotational jumps ($+\beta \leftrightarrow -\beta$ degrees) around its y axis with a first order rate constant, k_r (*SI Appendix, Section S10*). In the language of magnetic resonance, this rocking motion constitutes a “symmetric two-site exchange” process (45), the effect of which is to modulate the hyperfine field experienced by the electron spin. For a given set of anisotropic hyperfine interactions, the only additional parameters are the rocking angle and the rate constant.

To get an initial idea of the expected behavior, we started with the toy radical pair introduced above. Fig. 3A shows Φ_S when Y^\bullet is stationary and X^\bullet undergoes 10° rotational jumps (i.e., $\beta = 5^\circ$)

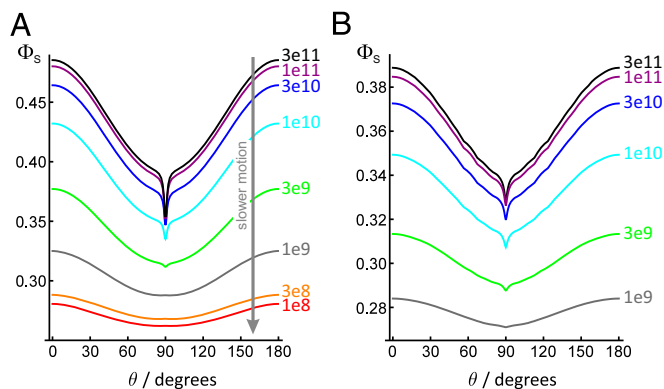


Fig. 3. Reaction yields of radical pairs with spin relaxation included. (A) The toy radical pair, $[\text{X}^\bullet \text{Y}^\bullet]$. X^\bullet has a single ^{14}N nucleus with hyperfine components (A_{xx}, A_{yy}, A_{zz}) = $(-0.2, -0.2, 1.7569)$ mT; Y^\bullet has a single ^{14}N nucleus with hyperfine components $(0.0, 0.0, 1.0812)$ mT. The two hyperfine tensors have parallel z axes. The radical pair lifetime is 10 μs . X^\bullet underwent 10° rotational jumps (i.e., $\beta = 5^\circ$) around the y axis with rate constants k_r between 3×10^{11} and 10^8 s^{-1} , as indicated. (B) The $[\text{FAD}^{\bullet-} \text{Y}^\bullet]$ radical pair. $\text{FAD}^{\bullet-}$ has seven magnetic nuclei, as in Fig. 1. Y^\bullet has single ^{14}N nucleus with hyperfine components (A_{xx}, A_{yy}, A_{zz}) = $(0.0, 0.0, 1.0812)$ mT. The radical pair lifetime is 10 μs . $\text{FAD}^{\bullet-}$ underwent 10° rotational jumps (i.e., $\beta = 5^\circ$) around the y axis, with rate constants k_r varying between 3×10^{11} and 10^9 s^{-1} , as indicated. In A and B, the direction of the magnetic field (θ) is varied in the xz plane of the flavin ring system (Fig. 1A). Almost identical results were found for the zy plane.

around its y axis. The lifetime of the radical pair was fixed at 10 μs , so that any relaxation pathway occurring on this timescale, or faster, could influence Φ_S . When the rocking is sufficiently fast ($k_r \geq 3 \times 10^9 \text{ s}^{-1}$; Fig. 3A), the differences in the magnetic interactions in the two orientations are averaged by the motion and a single sharp spike is seen at $\theta = 90^\circ$. As k_r is reduced, the averaging becomes less efficient, causing attenuation of the spike (without significant broadening) and flattening of the gently varying background (Fig. 3A and *SI Appendix, Section S11*). Spin relaxation is most efficient when k_r is comparable to the strengths of the hyperfine interactions, i.e., $\sim 10^8 \text{ s}^{-1}$. Under these conditions, Φ_S tends toward 0.25, the statistical singlet fraction expected at thermal equilibrium.

These simulations were performed for a rocking axis (y) perpendicular to the symmetry axis (z) of the hyperfine tensor in X^\bullet . Rotation around an axis tilted out of the xy plane results in less extensive modulation of the magnetic interactions, less efficient spin relaxation, and less attenuation of the spike for a given k_r . In this respect, Fig. 3A represents the worst case. The behavior of Φ_S when $k_r \leq 10^8 \text{ s}^{-1}$ is discussed in *SI Appendix, Section S12*.

In summary, the spike survives if $k_r \geq 3 \times 10^9 \text{ s}^{-1}$ (Fig. 3A). This value corresponds to a librational wavenumber of the aromatic ring systems greater than $\sim 0.1 \text{ cm}^{-1}$.

Spin Relaxation in a Flavin-Containing Radical Pair. We now look at the effects of motion on a more realistic spin system. It proved impractical to repeat the above calculation for the full (16-spin) $[\text{FAD}^{\bullet-} \text{TrpH}^{\bullet+}]$ radical pair treated above. Instead, we studied $[\text{FAD}^{\bullet-} \text{Y}^\bullet]$ in which $\text{FAD}^{\bullet-}$ contained seven nuclear spins (as above) and Y^\bullet was the same as in the toy radical pair, $[\text{X}^\bullet \text{Y}^\bullet]$. Fig. 3B shows Φ_S for $[\text{FAD}^{\bullet-} \text{Y}^\bullet]$ with the $\text{FAD}^{\bullet-}$ radical undergoing 10° rotational jumps ($\beta = 5^\circ$) around its y axis with rate constants in the fast exchange regime: $10^9 \text{ s}^{-1} \leq k_r \leq 3 \times 10^{11} \text{ s}^{-1}$. As was the case for $[\text{X}^\bullet \text{Y}^\bullet]$ (Fig. 3A), when $\tau = 10 \mu\text{s}$, the spike at $\theta = 90^\circ$ persists for rocking rates down to $3 \times 10^9 \text{ s}^{-1}$ and is even visible when $k_r = 10^9 \text{ s}^{-1}$. Similar behavior was found for a $[\text{X}^\bullet \text{TrpH}^{\bullet+}]$ pair in which $\text{TrpH}^{\bullet+}$ underwent 10° jumps (*SI Appendix, Section S13*). Spin relaxation effects were more pronounced for jumps larger than 10° .

Clearly, the dynamics of $\text{FAD}^{\bullet-}$ and $\text{TrpH}^{\bullet+}$ in cryptochrome are considerably more complicated than this two-site jump model.

However, we can infer from these exploratory studies that the spike in Φ_S is not excessively sensitive to reasonably rapid, relatively low-amplitude motions of the type likely to occur for the radicals in their binding sites in cryptochrome. The message we take from these calculations is that radical motions on timescales faster than about 1 ns could allow the spikiness of Φ_S to survive.

Precision of the Compass Bearing. The directional information available from Φ_S will inevitably be degraded by stochastic noise in the detection system (46). We can anticipate that for a given noise level, a sharper and stronger spike will deliver a more precise compass bearing. In *SI Appendix, Section S14*, we attempt to quantify the effects of detector noise on the signals in Fig. 1. It is shown that to obtain a precision of 1° when $\tau = 1 \mu\text{s}$, the noise level would have to be ~ 40 times smaller than when $\tau = 10 \mu\text{s}$. If such an improvement in signal-to-noise had to be achieved by averaging repeated measurements, it would take $\sim 40^2 = 1,600$ times longer for a radical pair with a lifetime of $1 \mu\text{s}$ than for one with $10 \mu\text{s}$. Put another way, a bird might be able to obtain a $\pm 1^\circ$ compass bearing in, say, 1 s instead of 30 min or by using $\sim 1,600$ times fewer cryptochrome molecules, if τ were $10 \mu\text{s}$ rather than $1 \mu\text{s}$.

Discussion

We have demonstrated that a radical pair magnetoreceptor may be capable of much higher angular precision than previously thought possible. More specifically, we have presented a version of the radical pair model that could potentially explain the magnetic compass precision observed for night-migratory songbirds (32, 33). The feature that makes this feasible, referred to as a spike, emerges naturally for cryptochrome-based radical pairs when the lifetime of the spin coherence exceeds $1 \mu\text{s}$.

FAD Radical. A fundamental requirement for the occurrence of a pronounced spike in the reaction yield (Φ_S) is that one of the radicals is $\text{FAD}^{\bullet-}$ or at least something closely resembling it. In particular, the two nitrogen nuclei (N5 and N10) in the central ring of the tricyclic flavin ring system appear to have almost ideal magnetic hyperfine interactions (16). The width and height of the spike can be tuned by adjusting the transverse components (A_{xx} and A_{yy}) of these interactions (some experimental values are given in *SI Appendix, Section S7*), implying that random mutations in the sequence of the protein in the neighborhood of the FAD could have provided evolution with the scope to optimize the compass precision. We emphasize that the precise values of the hyperfine parameters required to produce a substantial spike in Φ_S are not crucial and were neither guessed nor carefully chosen; they came directly from independent molecular orbital calculations (performed several years before we embarked on the present work) (47).

Partner Radical. A second prerequisite for spiky behavior is that the radical that partners the $\text{FAD}^{\bullet-}$ must have at least one appreciably anisotropic hyperfine interaction. This condition is certainly satisfied by the $\text{TrpH}^{\bullet+}$ radical formed by photo-induced electron transfer along the Trp-triad in cryptochrome, as our simulations demonstrated. It is also consistent with the oxidized form of ascorbic acid ($\text{Asc}^{\bullet-}$), a radical that has been tentatively suggested (but for which there is currently no evidence) as an alternative to $\text{TrpH}^{\bullet+}$, on the basis that $[\text{FAD}^{\bullet-} \text{Asc}^{\bullet-}]$ is expected to show much larger magnetic field effects than $[\text{FAD}^{\bullet-} \text{TrpH}^{\bullet+}]$ by virtue of the small hyperfine interactions in $\text{Asc}^{\bullet-}$ (16) (see ref. 16 for a more detailed discussion of possible partner radicals). However, a spike would not be expected for a $[\text{FAD}^{\bullet-} \text{Z}^{\bullet}]$ radical pair, in which Z^{\bullet} is a radical completely devoid of hyperfine interactions, such as superoxide, $\text{O}_2^{\bullet-}$ (even if its spin relaxation could be made slow enough) (48, 49). Such a radical pair was originally proposed to explain the reported inability of European robins (*Erithacus rubecula*) to use their magnetic compass when exposed to a narrow-band radiofrequency field at the Larmor frequency (1.4 MHz for a $50\text{-}\mu\text{T}$ geomagnetic field) (50). However,

very recent experiments (51), designed to replicate the earlier study (50), under much more stringently controlled conditions, failed to find specific effects at the Larmor frequency. In contrast, very weak broadband fields were found to disrupt the birds' magnetic compass orientation capabilities (51, 52). These new findings are consistent with radical pairs that have significant hyperfine interactions in both radicals, e.g., $[\text{FAD}^{\bullet-} \text{TrpH}^{\bullet+}]$ and $[\text{FAD}^{\bullet-} \text{Asc}^{\bullet-}]$.

Spin Relaxation and Magnetic Disorientation. The third major condition for the emergence of the spike is that the spin coherence times of the radicals should be longer than $1 \mu\text{s}$, which in turn means that the librations of the radicals within their binding pockets must be of relatively low amplitude and not too sluggish. As such motions are determined by the interactions of the radicals with the protein environment, this is another property that could have been optimized by evolution. Spin relaxation much slower than $1 \mu\text{s}$ has been invoked before to explain the apparent sensitivity of birds to weak (nanotesla) monochromatic radiofrequency fields (21, 26, 53, 54). The problem with this proposal is that if there is no possibility of a spike, a coherence time of $1\text{--}2 \mu\text{s}$ is sufficient to achieve the optimum compass performance so that there would be no evolutionary pressure to prolong relaxation times beyond this point (55, 56). Because the spike only emerges when the coherence time exceeds $1 \mu\text{s}$, its presence could explain why slow relaxation might have evolved. Moreover, it may now become possible to understand how radiofrequency fields, in particular broadband anthropogenic electromagnetic noise (sometimes called electrosmog) (52), interferes with the operation of the avian compass: not because all anisotropy is destroyed (21), but because the spike is attenuated. It remains to be seen, however, whether the spin relaxation can be slow enough to explain the reported effects (52).

Experimental Evidence. How could one determine whether a spike is really responsible for the precision of the avian magnetic compass? Although direct detection might be challenging, it should be possible to discover whether conditions could exist in a cryptochrome that would be compatible with the existence of a spike. Once it has been established which of the four known avian cryptochromes (13) plays a role in compass magnetoreception, and its structure is known, it will be possible to determine more about the librational motions of the radicals and the spin relaxation they produce. It seems probable that the magnetic and dynamic properties of a cryptochrome that has evolved as a compass sensor would differ significantly from those of cryptochromes that do not have a magnetic sensing function. It also appears likely that the properties of such a protein in vivo will differ from those of the isolated protein in vitro, for example, as a result of binding to signaling partners or attachment to whatever intracellular structures are responsible for alignment and/or immobilization of the protein (28).

Another approach would be to extend the behavioral experiments mentioned above in which broadband subnanotesla electromagnetic noise was found to prevent European robins from using their magnetic compass (52). If, for example, the birds' ability to orient was disrupted by 1- to 100-kHz but by not 1- to 10-kHz broadband noise, this would provide evidence for radical pair lifetimes and spin relaxation times in the range of $10\text{--}100 \mu\text{s}$ (50).

Quantum Biology. The radical pair mechanism of magnetoreception has found a place in the emerging field of Quantum Biology (57–59) on the strength of the absolute requirement that the radical pair must be in a coherent superposition of the quantum states of the two electron spins. In fact, the initial electronic singlet state of the radical pair is quantum mechanically entangled [although the entanglement, as such, confers no advantage in terms of the general operation of the compass (60), nor is it essential for the existence of the spike]. We recently showed that the spin dynamics of long-lived radical pairs in weak

magnetic fields can be described by a semiclassical approximation that becomes increasingly accurate as the number of nuclear spins is increased (61, 62). If the behavior of a realistic radical pair magnetoreceptor can be satisfactorily modeled in terms of classical rather than quantum oscillations, then arguably it does not belong under the quantum biological umbrella. However, the spike discussed here is undeniably a quantum effect, arising from the mixing of states associated with avoided energy-level crossings, and is not captured by the semiclassical theory. In this

sense, radical pair magnetoreception may be more of a quantum phenomenon than hitherto realized.

ACKNOWLEDGMENTS. P.J.H. thanks Malcolm Levitt, Ulrich Steiner, and Stefan Weber for helpful discussions. We thank Ilia Solov'yov for comments on the manuscript. This work was supported by the European Research Council (ERC; under the European Union's 7th Framework Programme, FP7/2007-2013/ERC Grant 340451), the US Air Force (USAF) Office of Scientific Research (Air Force Materiel Command, USAF Award FA9550-14-1-0095), the Electromagnetic Fields Biological Research Trust, the Deutsche Forschungsgemeinschaft (GRK 1885), and the Volkswagenstiftung (Lichtenberg Professur).

1. Wiltschko W, Munro U, Ford H, Wiltschko R (1993) Red-light disrupts magnetic orientation of migratory birds. *Nature* 364(6437):525–527.
2. Mouritsen H, Feenders G, Liedvogel M, Wada K, Jarvis ED (2005) Night-vision brain area in migratory songbirds. *Proc Natl Acad Sci USA* 102(23):8339–8344.
3. Zapka M, et al. (2009) Visual but not trigeminal mediation of magnetic compass information in a migratory bird. *Nature* 461(7268):1274–1277.
4. Mouritsen H, Hore PJ (2012) The magnetic retina: Light-dependent and trigeminal magnetoreception in migratory birds. *Curr Opin Neurobiol* 22(2):343–352.
5. Heyers D, Manns M, Luksch H, Güntürkün O, Mouritsen H (2007) A visual pathway links brain structures active during magnetic compass orientation in migratory birds. *PLoS One* 2(9):e937.
6. Hein CM, et al. (2010) Night-migratory garden warblers can orient with their magnetic compass using the left, the right or both eyes. *J R Soc Interface* 7(Suppl 2): S227–S233.
7. Hein CM, Engels S, Kishkinev D, Mouritsen H (2011) Robins have a magnetic compass in both eyes. *Nature* 471(7340):E11–E12, discussion E12–E13.
8. Schulten K, Swenberg CE, Weller A (1978) A biomagnetic sensory mechanism based on magnetic field modulated coherent electron spin motion. *Z Phys Chem NF* 111(1):1–5.
9. Ritz T, Adem S, Schulten K (2000) A model for photoreceptor-based magnetoreception in birds. *Biophys J* 78(2):707–718.
10. Cintolesi F, Ritz T, Kay CWM, Timmel CR, Hore PJ (2003) Anisotropic recombination of an immobilized photoinduced radical pair in a 50- μ T magnetic field: A model avian photomagnetoceptor. *Chem Phys* 294(3):385–399.
11. Mouritsen H, et al. (2004) Cryptochromes and neuronal-activity markers colocalize in the retina of migratory birds during magnetic orientation. *Proc Natl Acad Sci USA* 101(39):14294–14299.
12. Rodgers CT, Hore PJ (2009) Chemical magnetoreception in birds: The radical pair mechanism. *Proc Natl Acad Sci USA* 106(2):353–360.
13. Liedvogel M, Mouritsen H (2010) Cryptochromes—A potential magnetoreceptor: What do we know and what do we want to know? *J R Soc Interface* 7(Suppl 2): S147–S162.
14. Niessner C, et al. (2011) Avian ultraviolet/violet cones identified as probable magnetoreceptors. *PLoS One* 6(5):e20091.
15. Maeda K, et al. (2012) Magnetically sensitive light-induced reactions in cryptochrome are consistent with its proposed role as a magnetoreceptor. *Proc Natl Acad Sci USA* 109(13):4774–4779.
16. Lee AA, et al. (2014) Alternative radical pairs for cryptochrome-based magnetoreception. *J R Soc Interface* 11(95):20131063.
17. Solov'yov IA, Chandler DE, Schulten K (2007) Magnetic field effects in *Arabidopsis thaliana* cryptochrome-1. *Biophys J* 92(8):2711–2726.
18. Lüdemann G, Solov'yov IA, Kubar T, Elstner M (2015) Solvent driving force ensures fast formation of a persistent and well-separated radical pair in plant cryptochrome. *J Am Chem Soc* 137(3):1147–1156.
19. Lau JCS, Rodgers CT, Hore PJ (2012) Compass magnetoreception in birds arising from photo-induced radical pairs in rotationally disordered cryptochromes. *J R Soc Interface* 9(77):3329–3337.
20. Cai J, Guerreschi GG, Briegel HJ (2010) Quantum control and entanglement in a chemical compass. *Phys Rev Lett* 104(22):220502.
21. Gauger EM, Rieper E, Morton JLL, Benjamin SC, Vedral V (2011) Sustained quantum coherence and entanglement in the avian compass. *Phys Rev Lett* 106(4):040503.
22. Bandyopadhyay JN, Paterek T, Kaszlikowski D (2012) Quantum coherence and sensitivity of avian magnetoreception. *Phys Rev Lett* 109(11):110502.
23. Dellis AT, Kominis IK (2012) The quantum Zeno effect immunizes the avian compass against the deleterious effects of exchange and dipolar interactions. *Biosystems* 107(3):153–157.
24. Pauls JA, Zhang Y, Berman GP, Kais S (2013) Quantum coherence and entanglement in the avian compass. *Phys Rev E Stat Nonlin Soft Matter Phys* 87(6):062704.
25. Zhang Y, Berman GP, Kais S (2014) Sensitivity and entanglement in the avian chemical compass. *Phys Rev E Stat Nonlin Soft Matter Phys* 90(4):042707.
26. Xu BM, Zou J, Li H, Li JG, Shao B (2014) Effect of radio frequency fields on the radical pair magnetoreception model. *Phys Rev E Stat Nonlin Soft Matter Phys* 90(4):042711.
27. Carrillo A, Cornelio MF, de Oliveira MC (2015) Environment-induced anisotropy and sensitivity of the radical pair mechanism in the avian compass. *Phys Rev E Stat Nonlin Soft Matter Phys* 92(1):012720.
28. Solov'yov IA, Mouritsen H, Schulten K (2010) Acuity of a cryptochrome and vision-based magnetoreception system in birds. *Biophys J* 99(1):40–49.
29. Wiltschko W, Wiltschko R (1972) Magnetic compass of European robins. *Science* 176(4030):62–64.
30. Gill RE, et al. (2009) Extreme endurance flights by landbirds crossing the Pacific Ocean: Ecological corridor rather than barrier? *Proc Biol Sci* 276(1656):447–457.
31. Cochran WW, Mouritsen H, Wikelski M (2004) Migrating songbirds recalibrate their magnetic compass daily from twilight cues. *Science* 304(5669):405–408.
32. Akesson S, Morin J, Muheim R, Ottosson U (2001) Avian orientation at steep angles of inclination: Experiments with migratory white-crowned sparrows at the magnetic North Pole. *Proc Biol Sci* 268(1479):1907–1913.
33. Lefeldt N, Dreyer D, Schneider NL, Steenken F, Mouritsen H (2015) Migratory black-caps tested in Emlen funnels can orient at 85 degrees but not at 88 degrees magnetic inclination. *J Exp Biol* 218(Pt 2):206–211.
34. Timmel CR, Cintolesi F, Brocklehurst B, Hore PJ (2001) Model calculations of magnetic field effects on the recombination reactions of radicals with anisotropic hyperfine interactions. *Chem Phys Lett* 334(4-6):387–395.
35. Lau JCS, Wagner-Rundell N, Rodgers CT, Green NJB, Hore PJ (2010) Effects of disorder and motion in a radical pair magnetoreceptor. *J R Soc Interface* 7(Suppl 2):S257–S264.
36. Timmel CR, Till U, Brocklehurst B, McLaughlan KA, Hore PJ (1998) Effects of weak magnetic fields on free radical recombination reactions. *Mol Phys* 95(1):71–89.
37. Till U, Timmel CR, Brocklehurst B, Hore PJ (1998) The influence of very small magnetic fields on radical recombination reactions in the limit of slow recombination. *Chem Phys Lett* 298(1-3):7–14.
38. Efimova O, Hore PJ (2008) Role of exchange and dipolar interactions in the radical pair model of the avian magnetic compass. *Biophys J* 94(5):1565–1574.
39. Giovani B, Byrdin M, Ahmad M, Brettel K (2003) Light-induced electron transfer in a cryptochrome blue-light photoreceptor. *Nat Struct Biol* 10(6):489–490.
40. Zeugner A, et al. (2005) Light-induced electron transfer in *Arabidopsis* cryptochrome-1 correlates with *in vivo* function. *J Biol Chem* 280(20):19437–19440.
41. Biskup T, et al. (2009) Direct observation of a photoinduced radical pair in a cryptochrome blue-light photoreceptor. *Angew Chem Int Ed Engl* 48(2):404–407.
42. Zoltowski BD, et al. (2011) Structure of full-length *Drosophila* cryptochrome. *Nature* 480(7377):396–399.
43. Levy C, et al. (2013) Updated structure of *Drosophila* cryptochrome. *Nature* 495(7441): E3–E4.
44. Cai JM, Caruso F, Plenio MB (2012) Quantum limits for the magnetic sensitivity of a chemical compass. *Phys Rev A* 85(4):040304.
45. Hore PJ (2015) *Nuclear Magnetic Resonance* (Oxford Univ Press, Oxford, UK).
46. Weaver JC, Vaughan TE, Astumian RD (2000) Biological sensing of small field differences by magnetically sensitive chemical reactions. *Nature* 405(6787):707–709.
47. Rodgers CT (2007) Magnetic field effects in chemical systems. DPhil thesis (Univ of Oxford, Oxford, UK).
48. Hogben HJ, Efimova O, Wagner-Rundell N, Timmel CR, Hore PJ (2009) Possible involvement of superoxide and dioxygen with cryptochrome in avian magnetoreception: origin of Zeeman resonances observed by *in vivo* EPR spectroscopy. *Chem Phys Lett* 480(1-3):118–122.
49. Solov'yov IA, Schulten K (2009) Magnetoreception through cryptochrome may involve superoxide. *Biophys J* 96(12):4804–4813.
50. Ritz T, et al. (2009) Magnetic compass of birds is based on a molecule with optimal directional sensitivity. *Biophys J* 96(8):3451–3457.
51. Schwarze S, et al. (2016) Weak broadband electromagnetic fields are more disruptive to magnetic compass orientation in a night-migratory songbird (*Erithacus rubecula*) than strong narrow-band fields. *Front Behav Neurosci*, 10.3389/fnbeh.2016.00055.
52. Engels S, et al. (2014) Anthropogenic electromagnetic noise disrupts magnetic compass orientation in a migratory bird. *Nature* 509(7500):353–356.
53. Kavokin KV (2009) The puzzle of magnetic resonance effect on the magnetic compass of migratory birds. *Bioelectromagnetics* 30(5):402–410.
54. Gauger EM, Benjamin SC (2013) Comment on “Quantum coherence and sensitivity of avian magnetoreception”. *Phys Rev Lett* 110(17):178901.
55. Stoneham AM, Gauger EM, Porfyrakis K, Benjamin SC, Lovett BW (2012) A new type of radical-pair-based model for magnetoreception. *Biophys J* 102(5):961–968.
56. Lambert N, De Liberato S, Emary C, Nori F (2013) Radical-pair model of magnetoreception with spin-orbit coupling. *New J Phys* 15(8):083024.
57. Ball P (2011) Physics of life: The dawn of quantum biology. *Nature* 474(7351):272–274.
58. Al-Khalili J, McFadden J (2014) *Life on the Edge: The Coming of Age of Quantum Biology* (Bantam Press, London).
59. Solov'yov IA, Ritz T, Schulten K, Hore PJ (2014) A chemical compass for bird navigation. *Quantum Effects in Biology*, eds Mohseni M, Omar Y, Engel GS, Plenio MB (Cambridge Univ Press, Cambridge, UK), pp 218–236.
60. Hogben HJ, Biskup T, Hore PJ (2012) Entanglement and sources of magnetic anisotropy in radical pair-based avian magnetoreceptors. *Phys Rev Lett* 109(22):220501.
61. Manolopoulos DE, Hore PJ (2013) An improved semiclassical theory of radical pair recombination reactions. *J Chem Phys* 139(12):124106.
62. Lewis AM, Manolopoulos DE, Hore PJ (2014) Asymmetric recombination and electron spin relaxation in the semiclassical theory of radical pair reactions. *J Chem Phys* 141(4): 044111.